Chemical Science

EDGE ARTICLE

View Article Online
View Journal | View Issue

Cite this: *Chem. Sci.*, 2018, **9**, 3584

A "waiting" carbon nitride radical anion: a charge storage material and key intermediate in direct C–H thiolation of methylarenes using elemental sulfur as the "S"-source†

Aleksandr Savateev,*[a] Bogdan Kurpil,[a] Artem Mishchenko,[b] Guigang Zhang[a] and Markus Antonietti[a]

Received 13th February 2018
Accepted 9th March 2018

DOI: 10.1039/c8sc00745d

rsc.li/chemical-science

Potassium poly(heptazine imide), a carbon nitride based semiconductor with high structural order and a valence band potential of +2.2 V *vs.* NHE, in the presence of hole scavengers and under visible light irradiation gives the corresponding polymeric radical anion, in which the specific density of unpaired electrons reaches 112 μmol g^{-1}. The obtained polymeric radical anion is stable under anaerobic conditions for several hours. It was characterized using UV-vis absorption, time resolved and steady state photoluminescence spectra. The electronic structure of the polymeric radical anion was confirmed by DFT cluster modelling. The unique properties of potassium poly(heptazine imide) for storing charges were employed in visible light photocatalysis. A series of substituted dibenzyldisulfanes was synthesized in 41–67% yield from the corresponding methylarenes *via* cleavage of the methyl C–H bond under visible light irradiation and metal-free conditions.

Introduction

C–H functionalization of hydrocarbons mediated by heterogeneous visible light photocatalysts is highly attractive for sustainable chemistry.[1] This strategy can afford high value-added chemicals from inexpensive reagents, minimize the number of steps and hence auxiliary chemicals, reduce the number of by-products and could potentially use only sunlight as the energy source, while the photocatalyst can be easily separated from the solution and used again.[2] Numerous examples of heterogeneous photocatalysts and photocatalytic reactions have been reported in the literature – the hydrogen evolution reaction[3,4] and overall water splitting,[5] CO_2 reduction[6,7] and styrene production, just to name a few.[8] Due to their chemical inertness, arising from very high C–H bond energies and ionization potentials, selective functionalization of hydrocarbons is quite challenging.[9]

The literature, describing C–H functionalization of hydrocarbons mediated by heterogeneous photocatalysts, is mostly represented by synthesis of aldehydes, ketones and carboxylic acids, since O_2 in all these cases is used as an electron scavenger and hydrogen oxidation as the thermodynamic driving force.[10–13]

In order to transcend the borders of heterogeneous photocatalysis applied to organic synthesis and to broaden the spectrum of products, semiconductors with high oxidation power of photogenerated holes may be envisioned for use. According to this strategy, a potent thermodynamic driving force for substrate oxidation is created, eliminating the need for O_2, while mild electron acceptors can then be used to remove the electron from the conduction band (CB) and close the photocatalytic cycle.

In this regard, potassium poly(heptazine imide), K-PHI hereafter (Fig. 1a),[14] a carbon nitride based material, is a promising candidate to assay this strategy.[15–17] The band structure of K-PHI is schematically shown in Fig. 1d. Due to the highly positive valence band (VB) potential, +2.22 V *vs.* NHE, photogenerated holes are effective oxidants for application in organic synthesis. For example, K-PHI was successfully used in the oxidation of alcohols to aldehydes and 1,4-dihydropyridines to pyridines,[18] in the synthesis of 1,3,4-oxadizoles by oxidative cyclization of *N*-acylhydrazones,[19] in thioamide synthesis by photocatalytic Kindler reaction,[20] and in oxygen and hydrogen evolution reactions.[21]

On the other hand, the CB in K-PHI is located at −0.5 V *vs.* NHE, which is significantly lower compared, for example, to that of graphitic carbon nitride (g-CN), −1.29 V *vs.* NHE. Therefore, it is reasonable to assume that the K-PHI radical anion, hereafter denoted as K-PHI$^{\bullet-}$, formed from K-PHI upon its single electron

[a]*Department of Colloid Chemistry, Max-Planck Institute of Colloids and Interfaces, Am Mühlenberg 1, 14476 Potsdam, Germany. E-mail: oleksandr.savatieiev@mpikg.mpg.de*

[b]*Department for Heterophase Synthesis of Inorganic Compounds and Materials, V.I. Vernadsky Institute of General and Inorganic Chemistry, Palladina Ave., 32/34, Kiev, 03142, Ukraine*

† Electronic supplementary information (ESI) available: XPS, UPS and FT-IR spectra of K-PHI, N_2 absorption isotherm, DFT calculations, toluene oxidative thiolation optimization results, material characterization after photocatalytic tests, and ^{1}H and ^{13}C NMR spectra of disulfanes. See DOI: 10.1039/c8sc00745d

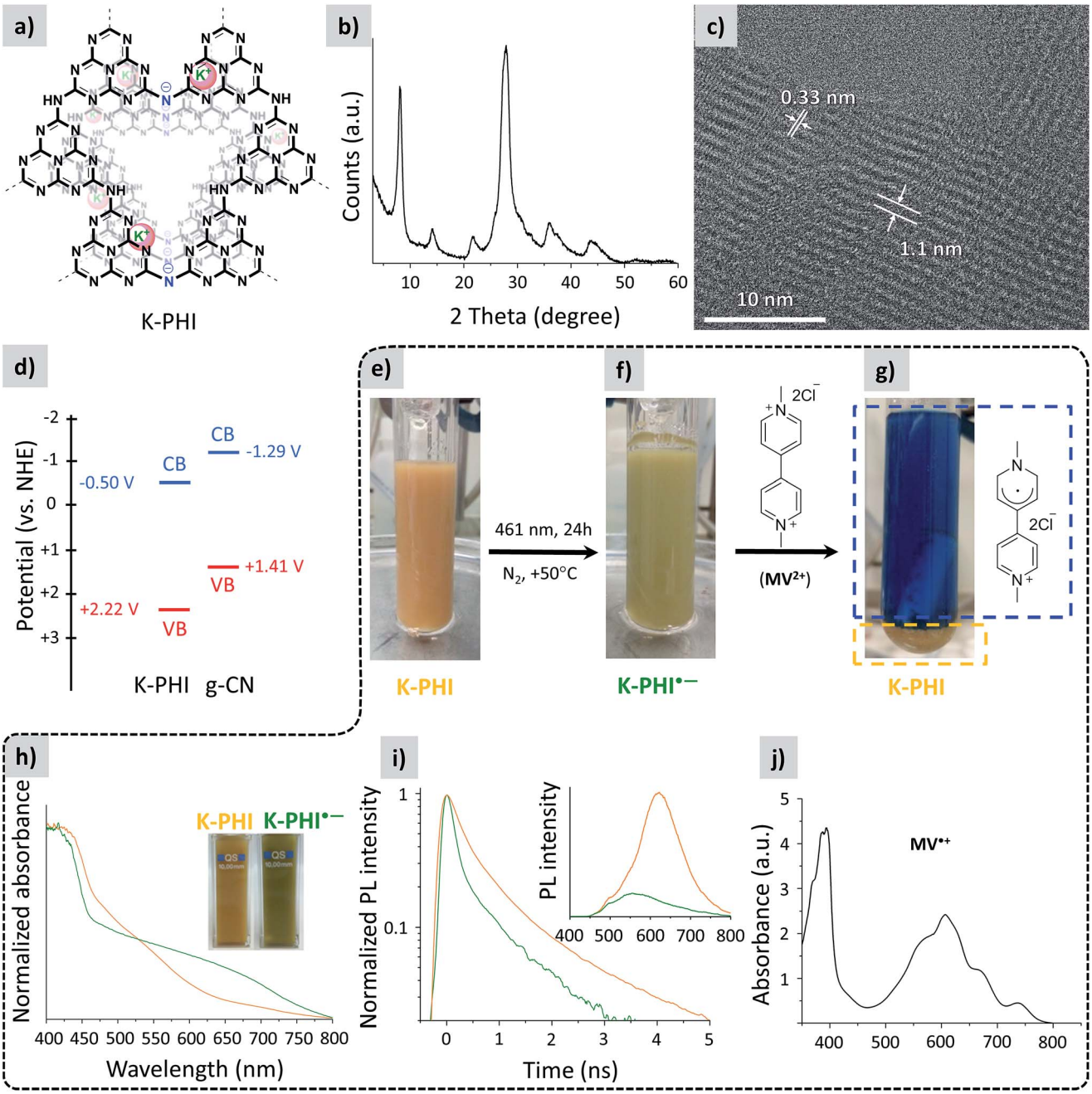

Fig. 1 (a) Idealized structure of K-PHI. (b) PXRD pattern of K-PHI. (c) HR-TEM image of K-PHI. (d) Band structure of K-PHI. The CB position of K-PHI was determined by Mott–Schottky analysis[15] and the VB position calculated as $E_{VB} = E_{CB}$ + BG, where BG is the optical band gap of K-PHI determined from the Tauc plot (Fig. S1e†). CB and VB potentials of g-CN were taken from the literature.[14] (e) Suspension of K-PHI (10.39 mg) and 4-methylanisole (0.6 mL) in acetonitrile (6.05 mL). (f) The same suspension after stirring at +50 °C for 24 h under light irradiation (461 nm, $0.0517 \pm 3 \times 10^{-5}$ W cm^{-2}). (g) The same suspension immediately after methylviologen dichloride dihydrate (6.9 mg, 24 μmol) addition. The blue rectangle shows the solution of $MV^{\bullet+}$ in acetonitrile, and the orange rectangle shows the precipitated K-PHI. (h) UV-vis absorption spectra of the K-PHI suspension in a 4-methylanisole/MeCN mixture: prior to irradiation (orange, the suspension appearance is also shown in (e)) and after irradiation for 2 h with a 461 nm LED (green, the suspension appearance is also shown in (f)), both recorded under anaerobic conditions. (i) Time resolved PL spectra of the K-PHI suspension in a 4-methylanisole/MeCN mixture: prior to irradiation (orange, the suspension appearance is also shown in (e)) and after irradiation for 2 h with a 461 nm LED (green, the suspension appearance is also shown in (f)), both recorded under anaerobic conditions. The steady state PL spectra of the suspended materials, recorded using a 360 nm excitation wavelength, are given as the inset. Experiments aimed at checking the ability of K-PHI to store electrons without any external energy input under anaerobic conditions are enclosed with a dashed line. (j) Absorption spectrum of $MV^{\bullet+}$ solution in acetonitrile.

reduction, would be stable and have a lifetime above the μs–s timescale (Fig. 2).[22] The viability of this idea was recently proved by Lotsch *et al.* who have reported radical carbon nitride species with a lifetime exceeding hours, while the material was applied in the hydrogen evolution reaction and a sunlight harvesting device.[23,24]

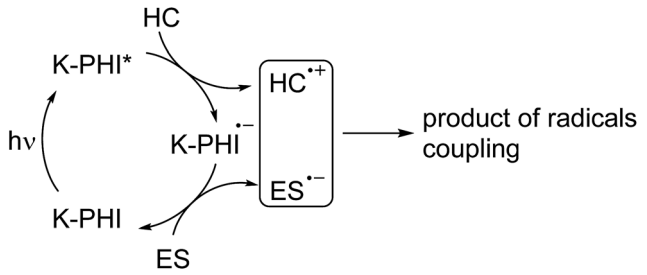

Fig. 2 A schematic representation of the photocatalytic reaction proceeding *via* reductive quenching of the photocatalyst. K-PHI* represents the excited state of the photocatalyst, K-PHI$^{\bullet-}$ stands for the radical anion, HC stands for "hydrocarbon", and ES stands for electron scavenger.

In view of hydrocarbon C–H bond activation, the long living K–PHI$^{\bullet-}$ might be a key intermediate permitting employment of reagents different from the abovementioned O_2. The mechanism describing this approach is summarized in Fig. 2.

In the present work, we have shown that K-PHI in the presence of hole scavengers, even those as weak as toluene, when triggered by visible light, acts as a capacious electron buffer and forms a stable radical anion under air-free conditions. This feature was applied in visible light photocatalytic activation of the C–H bond of hydrocarbons – we have developed a simple and convenient method to synthesize dibenzyldisulfanes from inexpensive methylarenes and S_8 under visible light irradiation using K-PHI as a heterogeneous photocatalyst under metal-free conditions.

Results and discussion

K-PHI was prepared according to a procedure reported by us earlier.[18] The powder X-ray (PXRD) pattern shows diffraction peaks typical of this material.[25] Among them, the intense peak at ~27° is due to stacking of layers similar to g-CN, and the peaks at 8.1°, 14.2°, 21.8°, 36.0° and 43.9° are related to an ordered in-layer arrangement (Fig. 1b).[25] The high resolution TEM image reveals the crystalline structure of the synthesized K-PHI with interlayer distances of 0.33 nm and an in-plane periodicity of 1.1 nm (Fig. 1c). The X-ray photoelectron, ultraviolet photoelectron, diffuse reflectance UV-vis absorption, photoluminescence, and Fourier-transform infrared (FT-IR) spectra, N_2 absorption isotherm and SEM image of K-PHI are given in the ESI (Fig. S1†) and they are consistent with those reported previously.[14,26,27]

In order to check the possibility of using K-PHI as an electron buffer and subsequently applying it in photocatalytic hydrocarbon functionalization, we performed the following experiment. A mixture of K-PHI and *p*-methylanisole (holes scavenger) in acetonitrile was mixed, degassed and kept under a N_2 atmosphere throughout the course of the experiment (Fig. 1e).‡ The suspension was irradiated with a 461 nm LED. After irradiation was stopped, we noticed that the suspended particles of K-PHI had changed colour from orange to "avocado green" (Fig. 1f). The colour change was taken as the first piece of evidence of K-PHI radical anion formation, hereafter denoted as K-PHI$^{\bullet-}$.[23] Upon addition of excess dimethylviologen dichloride dihydrate (MV^{2+}), yellow K-PHI immediately precipitated, while the solution changed its colour to intense blue, which is due to MV^{2+} single electron reduction to its radical cation ($MV^{\bullet+}$) (Fig. 1g). Measuring the absorbance of the solution at λ = 606 nm (Fig. 1j) and taking into account the extinction coefficient of $MV^{\bullet+}$ in acetonitrile of ε = 13 900,[28] the specific number of electrons stored by the polymeric K-PHI$^{\bullet-}$ was calculated to be 112 μmol per gram of the material. In the control experiment, when MV^{2+} and K-PHI were mixed together prior to irradiation, no $MV^{\bullet+}$ was formed. However, MV^{2+} was converted into $MV^{\bullet+}$ upon subsequent light irradiation. This implies that energy input is essential to enabling electron flux. Note that the capacity of the covalent g-CN in the same experiment was orders of magnitude lower.

The optical properties of the suspended K-PHI$^{\bullet-}$ (Fig. 1f) were investigated. The UV-vis absorption spectrum (Fig. 1h) shows a broad absorption band in the 600–750 nm range, which is in agreement with the observed green colour. The photoluminescence (PL) lifetime of K-PHI$^{\bullet-}$ is 0.35 ns *versus* 0.66 ns for K-PHI (Fig. 1i). The room temperature steady-state PL spectrum of the K-PHI$^{\bullet-}$ suspension is significantly lower compared to that of K-PHI in the ground state, while the maximum is shifted to a shorter wavelength (555 nm). This observation supports that *p*-methylanisole indeed acts as a hole scavenger – it depopulates the number of holes and hence reduces PL.

We observed a colour change of the suspension from green back to yellow when the suspension was exposed to S_8 or O_2 implying that these molecules can be used in combination with K-PHI in the subsequent functionalization of hydrocarbons (shown below).

In order to characterize theoretically the electronic structure of K-PHI, we conducted a density functional theory (DFT) study on a model K-PHI cluster containing 6 heptazine units and 2 potassium ions. Its geometry was optimized using several pure (PBE and BLYP) and hybrid (PBE0, B3LYP, and BHHLYP) generalized gradient approximation (GGA) functionals (see the Experimental section and ESI† for details).

To a first approximation the energies of the highest occupied (HOMO) and lowest unoccupied (LUMO) molecular orbitals of the model cluster can be compared with the edge energies of K-PHI valence and conduction bands respectively. These orbitals are of π-type and are located mainly on the nitrogen atoms of the poly(heptazine imide) matrix (Fig. 3). Among the functionals used, B3LYP gave the best agreement with the optical band gap determined experimentally, 3.02 eV *vs.* 2.72 eV (Table 1). On the other hand, PBE0 revealed that the HOMO of the K-PHI cluster is located at +2.08 eV, which is comparable with the valence band position, +2.22 eV, obtained by adding the optical band gap value, 2.72 eV (Fig. S1e†), to the conduction band value, −0.5 eV. Moreover, this valence band position agrees well with the VBM, +2.40 eV, determined directly using ultraviolet photoelectron spectroscopy (UPS) (Fig. S1d†). Since the HOMO position is slightly more positive than the oxidation potential of toluene (or even more positive than that of *p*-

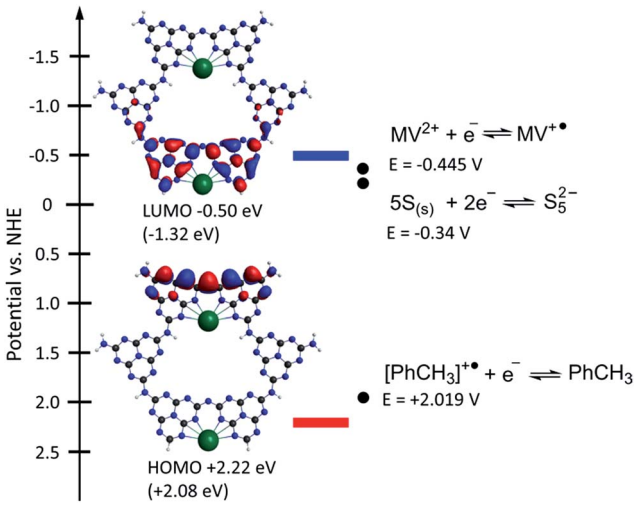

Fig. 3 CB position determined by Mott–Schottky analysis[15] and VB position calculated as $E_{VB} = E_{CB}$ + BG, where BG is the optical band gap, 2.72 eV, of K-PHI determined from the Tauc plot (Fig. S1e†). HOMO and LUMO positions in the K-PHI cluster predicted by the PBE0 functional are given for comparison in parentheses. HOMO and LUMO positions from Table 1 were recalculated taking into account an absolute value of $V_{NHE} = 4.18$ V for the normal hydrogen electrode. The standard oxidation potential of toluene, MV^{2+} and sulfur was adapted from the literature.[29–31]

Table 1 Computed orbital energies for the K-PHI cluster (eV in the absolute vacuum scale)

Value	PBE	PBE0	BLYP	B3LYP	BHHLYP
E_{HOMO}	−5.33	−6.26	−5.17	−5.99	−7.13
E_{LUMO}	−3.62	−2.86	−3.48	−2.97	−1.90
$\Delta E_{HOMO-LUMO}$	1.71	3.40	1.69	3.02	5.22

methylanisole, due to the M+ effect of the OMe group), electron transfer from toluene to the valence band of K-PHI is thermodynamically allowed (Fig. 3). On the other hand, the predicted LUMO position is −1.32 eV and is significantly more negative than the CB potential, −0.5 eV, measured using Mott–Schottky analysis.[15] Nevertheless, the reduction potential of MV^{2+} to $MV^{\bullet+}$, −0.445 V, is less negative than the CB potential; therefore flux of electrons from the CB of K-PHI to MV^{2+} is thermodynamically allowed.

The model reaction of K–$PHI^{\bullet-}$ quenching by adding MV^{2+}, O_2 or S_8 allows us to call K-PHI a "waiting" photocatalyst, because in the presence of a hole scavenger, even a weak one such as *p*-methylaniosle, and light energy input, it is rapidly converted into stable K-$PHI^{\bullet-}$ and "waits" until an oxidant comes to recover the ground state of K-PHI.

Having evidence that K-PHI is a capacious electron buffer and hence can decouple oxidation and reduction of the substrates, we applied this material in photocatalytic thiolation of toluene. Instead of using sulfur-transferring reagents, we took aim at elemental sulfur (S_8) as a cheap raw source. Its redox chemistry is well known and the problem of its utilization exists – the annual excess of sulfur production is about seven millions ton.[32] Instead of simply storing it, chemists are searching for possibilities to utilize this huge excess of sulfur as an alternative feedstock for polymeric materials,[33] as an electron sacrificial agent in photocatalysis[18] and so forth.[34] Toluene, having an oxidation potential of +2.019 ± 0.02 V (*vs.* NHE) and a relatively reactive methyl group,[29] has been chosen as a model substrate to screen the reaction conditions. The main results of these tests are summarized in Tables S1 and S2.† The formation of dibenzyldisulfide was unambiguously proved by the fact that its ^{13}C NMR, FT-IR and mass spectra were identical to those of the reference (Fig. S2†).

The developed photocatalytic system is indeed versatile and tolerant to different functional groups. A series of substituted methylarenes was converted into the corresponding disulfanes (Fig. 4). Dibenzyldisulfane **1a** was obtained in 56% isolated yield, while *p*-methoxysubstituted disulfane **1b** was obtained with even higher, 67%, yield. Interestingly, that steric effect is negligible and 1,2-bis(2-methoxybenzyl)disulfane **1c** was isolated with 63% yield. Ethylbenzene was exclusively oxidized at the α-position of the alkyl chain furnishing disulfane **1d**. This result again supports the idea that upon oxidation of alkylarene by K-PHI, first reactive species of benzyl-type is formed, which subsequently reacts with sulfur. Disulfane **1d** was isolated as a 1 : 1 mixture of its diastereomers as proven by ^{13}C NMR because K-PHI does not possess chirality. *p*-fluorotoluene was oxidized to disulfane **1e** with 41% isolated yield. *tert*-Butyl *p*-tolylcarbamate gave the corresponding disulfane **1f** with 51% isolated yield implying that K-PHI offers quite mild conditions, under which the protection group remains intact. In the case of *p*-toluonitrile the yield of disulfane **1g** was 9%, because the reaction terminated at the stage of polysulfane formation (see below). Finally, *p*-iodotoluene gave disulfane **1h**, though with *ca.* 3% yield, apparently due to lability of the C–I bond under photoredox conditions.

The highest yield of 1,2-dibenzyldisulfane was obtained when toluene oxidation was conducted under blue (461 nm)

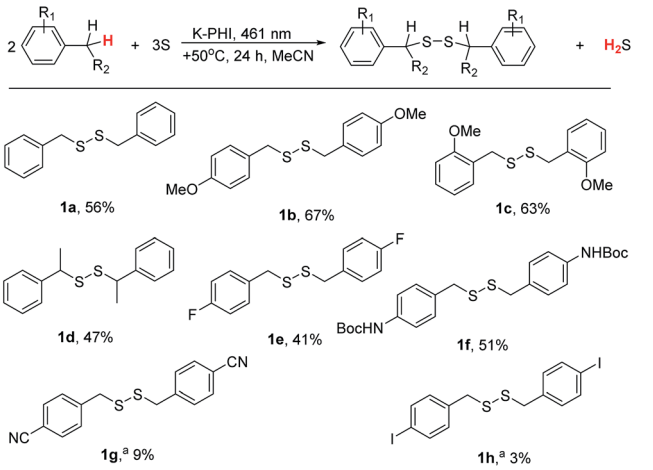

Fig. 4 Diaryldisulfane synthesis. Isolated yields are given unless otherwise specified. Conditions: K-PHI 10 mg, methylarene 0.3 mL, S_8 0.96 mg, MeCN 2.7 mL, +50 °C, 24 h, 461 nm ($0.0517 \pm 3 \times 10^{-5}$ mW cm^{-2}). [a] Determined by ^1H NMR using dibenzylether as an internal standard.

light (Fig. 5a), as this wavelength matches the K-PHI optical band gap, 2.72 eV. UV light (350 nm) gave disulfane with a slightly lower yield, which could be rationalized by consecutive S–S bond cleavage under the highly energetic UV radiation. On the other hand, under green light (522 nm) almost no disulfane was generated. The apparent quantum yield (AQY) of *p*-methylanisole photooxidation at 461 nm was calculated to be $0.23 \pm 0.02\%$ (Fig. 5a). Our calculations are based on the photon flux measured using an optical power meter equipped with an integrating sphere, taking into account that every polysulfane molecule requires oxidation of two *p*-methylanisole molecules. It indicates that C–H bond oxidation at close to room temperature is a difficult process especially in the absence of any metal co-catalysts, but still possible due to K-PHI.

All this behavior indicates that, in contrast to photochemical water splitting with g-CN, this time the reduction process is the slow, rate determining step, as there is obviously no straight chemical reaction channel for the sulfur to quickly take up the photogenerated electron to restore the ground state of the photoredox catalyst.

The Hammett plot (Fig. 5b) supports that the reaction is sensitive to electronic effects. The ρ constant is -0.75, suggesting that the rate limiting step involves positively charged species – the radical cation of benzyl type.

In the reaction mixture we detected intermediate polysulfanes, namely 1,4-bis(4-methoxybenzyl)tetrasulfane and 1,3-bis(4-methoxybenzyl)trisulfane, when oxidation of *p*-methylanisole was studied. Given that the chemical shift of the methylene groups depends on the number of sulfur atoms between the benzylic fragments, the peak at 4.13 ppm was assigned to the 1,4-bis(4-methoxybenzyl)tetrasulfane CH_2 group,[35] while the one at 4.01 ppm to the CH_2 group of 1,3-bis(4-methoxybenzyl)trisulfane[36] (Fig. 5c). The designed photocatalytic system can also produce polysulfides with up to 5 sulfur atoms when excess sulfur was used (Fig. S3†).

The time dependent composition of the reaction mixture is shown in Fig. 5d. Already after 86 min, 50% of sulfur was consumed. However, the yield of disulfane was only 30% of the theoretical value, suggesting that at the beginning of the reaction sulfur is rapidly converted into polysulfides and stored in the form of bis(4-methoxybenzyl)polysulfanes. Nevertheless, the intermediate tetra- and trisulfides were completely converted into 1,2-bis(4-methoxybenzyl)disulfane after *ca.* 27 h of irradiation, implying that disulfane is the most stable under the given photocatalytic conditions. The amount of target disulfane asymptotically approaches the theoretical value, expected for the given amount of sulfur, and after 44 h 93% of the maximum possible quantity was obtained, proving that the stoichiometric ratios between reagents and products are indeed as described in Fig. 4.

Summarizing all the abovementioned observations, the tentative mechanism of methylarene photocatalytic oxidative thiolation is shown in Fig. 6. Visible light excites K-PHI giving rise to K-PHI* species with a bound electron–hole exciton pair. At this point two pathways, oxidative and reductive quenching of K-PHI*, are in principle possible.[37] However, the reaction proceeds predominantly *via* the oxidation of methylarene (ArMe) to the corresponding radical cation ($ArMe^{\bullet+}$) which occurs relatively fast. The leftover $K\text{–}PHI^{\bullet-}$ is oxidized by S_8 back to the initial K-PHI, closing the photocatalytic cycle, while sulfur is then converted into $S_8^{\bullet-}$ (structure **a** on Fig. 6). We are aware that in solution sulfur can form polysulfides of different lengths as well as cyclic molecules,[38,39] but for clarity of presentation we assume that linear $S_8^{\bullet-}$ is the only product of sulfur reduction. Due to the positive charge, $ArMe^{\bullet+}$ is a much stronger acid ($pK_a = -13$, $PhCH_3^{\bullet+}$ in MeCN)[40] compared to the neutral ArMe ($pK_a = 54$, $PhCH_3$, in MeCN).[41]

On the other hand, $S_8^{\bullet-}$, similar to the well-studied trisulfur radical anion $S_3^{\bullet-}$,[42] is basic and therefore abstracts a proton

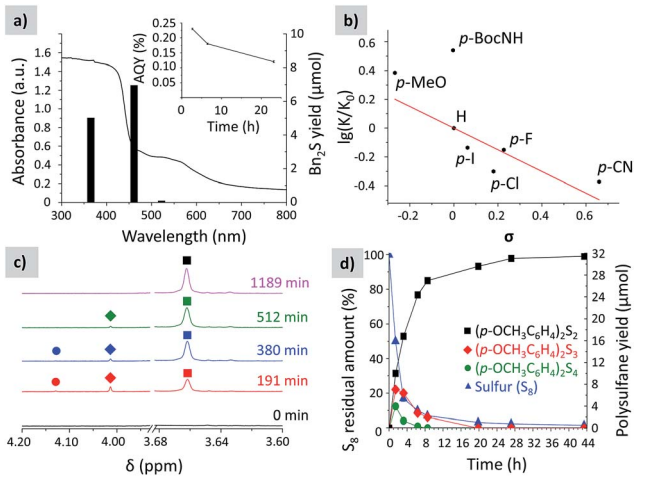

Fig. 5 (a) Diffuse reflectance UV-vis spectrum of K-PHI with the yield of 1,2-dibenzyldisulfane depending on the irradiation wavelength. (b) Hammett plot. (c) Time dependent evolution of the methylene group signal of $(p\text{-}OCH_3C_6H_4)_2S_2$ (squares), $(p\text{-}OCH_3C_6H_4)_2S_3$ (diamonds) and $(p\text{-}OCH_3C_6H_4)_2S_4$ (circles) in selected ^1H NMR spectra of the reaction mixture. (d) Time dependent yield of $(p\text{-}OCH_3C_6H_4)_2S_2$ (squares), $(p\text{-}OCH_3C_6H_4)_2S_3$ (diamonds) and $(p\text{-}OCH_3C_6H_4)_2S_4$ (circles), and residual sulfur (triangles).

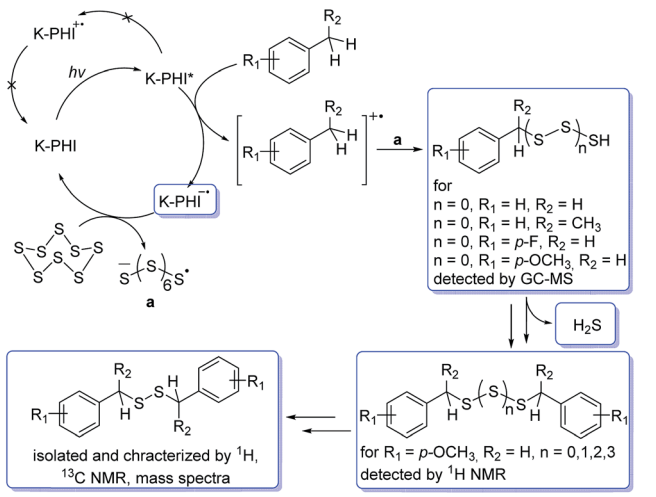

Fig. 6 A proposed mechanism of photocatalytic thiolation of toluene with elemental sulfur. Organic molecules or intermediate reactive species that were detected or isolated during the course of reaction are highlighted with rectangles.

from $ArMe^{\bullet+}$. This transfer produces $HS_8^{\bullet}$ and $ArCH_2^{\bullet}$ respectively. The formation of $ArCH_2^{\bullet}$ was proven indirectly – we observed 1,2-diphenylethane as a major product when toluene was used both as a reagent and a solvent (Table S1,† entries 2 and 9). In this case, the concentration of $ArCH_2^{\bullet}$ radicals becomes high enough to favour their recombination. In acetonitrile, in the next step a C–S bond is created by recombination between the $HS_8^{\bullet}$ and $ArCH_2^{\bullet}$ radicals. A transition of hydropolysulfides to disulfides requires evolution of H_2S and extrusion of extra sulfur atoms, which in turn participate in subsequent reactions with ArMe. Apparently, K-PHI is also involved in all these steps, *i.e.* the polysulfides obviously react similarly to the original sulfur reactant. H_2S was detected as Ag_2S, when the reaction mixture headspace was allowed to react with $AgNO_3$ (Fig. S4†). Also traces of intermediate RCH_2SH were detected by GC-MS of the reaction mixture additionally supporting the mechanism (mass spectra, Fig. S5†). Finally, the structure of K-PHI remains unaffected as proved by the identical nature of its PXRD patterns and FT-IR spectra before and after the photocatalytic experiment (Fig. S6†).

Conclusions

Potassium poly(heptazine imide) enables the photoredox thiolation of methylarenes with elemental sulfur. This reaction takes place under very mild conditions and blue light irradiation. The reaction proceeds *via* formation of polysulfides as intermediates, which potentially could also be isolated, if reaction is terminated at the appropriate time. The discovered photocatalytic conversion of methylarenes into disulfides clearly reflects the high oxidation power of K-PHI that activates the methyl C–H bond toward subsequent reaction with sulfur species. Mechanistic studies suggest that the reaction proceeds first *via* methylarene oxidation by the photogenerated hole of K-PHI*, leaving a $K\text{-}PHI^{\bullet-}$ radical anion. We isolated this long living $K\text{–}PHI^{\bullet-}$ radical anion and characterized it spectroscopically. The exceptionally long lifetime of the $K\text{-}PHI^{\bullet-}$ radical anion arises from its high stability under air-free conditions, as plausibilized by model calculations revealing a narrow band of delocalized states for the extra electron. All of this makes K-PHI a promising photo-responsive material for energy storage applications. The newly disclosed reaction is convenient for the generation of a number of technically very useful disulfanes, as they, for instance, are used for rubber processing, surface modifications, or click chemical modifications of (bio)polymers. We expect the reaction to be more general and applicable to the oxidative modification of all C–H positions where the cation radical is resonance stabilized.

Experimental section

^1H and ^{13}C NMR spectra were recorded on an Agilent 400 MHz spectrometer using the signal of TMS (0 ppm) as a reference. ^{13}C APT experiments were conducted to distinguish between C, CH_2 and CH, CH_3 carbon atoms. An Agilent 6890 Network GC System coupled with an Agilent 5975 Inert Mass Selective detector (electron ionization) was used for reaction mixture composition analysis and to obtain mass spectra of the products. Irradiance of the LED module was measured using a PM400 Optical Power and Energy Meter equipped with integrating sphere S142C.

Synthetic procedures

tert-Butyl *p*-tolylcarbamate was prepared according to a literature procedure.[43] Mesoporous graphitic carbon nitride (mpg-CN) was prepared according to a literature procedure.[44]

K-PHI was prepared according to a literature procedure.[18] A mixture of 5-aminotetrazole (0.99 g) and LiCl/KCl eutectics (4.97 g) was introduced into a steel ball mill cup. The steel ball was placed and the cup was closed. The mixture of precursors was ground for 5 min at a shaking rate of 25 s^{-1}. The resultant flour-like white powder was transferred into a porcelain crucible, covered with a porcelain lid and placed into an oven. The temperature inside the oven was increased from 20 °C to 600 °C within 4 hours under a flow of nitrogen (15 L min^{-1}) after which it was maintained at 600 °C for another 4 hours. The oven was allowed to cool to room temperature. The melt from the crucible was transferred into a beaker; deionized water (50 mL) and a stir bar were placed into the beaker. The suspension was kept stirring at room temperature for 4 hours until the suspension became fully homogeneous and no agglomerated particles were seen. The solid was separated by centrifugation (6500 min^{-1}, 12 min), washed with water (3 × 2 mL) using a centrifuge to separate particles of the material (13 500 min^{-1}, 1 min) and dried in a vacuum giving 256 mg of the dark-yellow material.

A general procedure of methylarene oxidative thiolation. A screw-capped tube was charged with K-PHI (10 mg), methylarene (0.3 mL), elemental sulfur (0.96 mg, 30 μmol of S atoms) and acetonitrile (2.7 mL). A Teflon coated stir bar was added as well. The suspension was frozen in liquid nitrogen to the solid state and evacuated until a residual pressure of 0.1 mbar was reached. The solid was warmed using a heating gun until the solid melted. The procedure was repeated 3 times and the tube was finally refilled with argon. The suspension was vigorously stirred at +50 °C under blue LED (461 nm, $0.0517 \pm 3 \times 10^{-5}$ W cm^{-2}) irradiation for 24 hours. The reaction mixture was allowed to cool to room temperature and the tube was opened in a fume hood. Attention! Evolution of H_2S! The catalyst was separated by centrifugation (13 000 min^{-1}) and washed with acetonitrile (3 × 1.5 mL). The washings were combined and acetonitrile was evaporated under reduced pressure (+50 °C, 80 mbar). The residue was washed with chloroform (3 × 2 mL) and undissolved particles were separated by centrifugation (13 000 min^{-1}). The evaporation of chloroform under reduced pressure furnished the corresponding disulfane.

1,2-Dibenzyldisulfane. Yield: 56%. The ^1H and ^{13}C NMR, and FT-IR spectra were identical to those of the authentic sample purchased from Acros Organics (Fig. S2†). ^1H NMR (400 MHz, $CDCl_3$): $\delta = 3.60$ (s, 4H, CH_2), 7.23–7.34 (m, 10H, CH). ^{13}C NMR (400 MHz, $CDCl_3$): $\delta = 43.2$ (s, CH_2), 127.4 (s, CH), 128.5 (s, CH), 129.4 (s, CH), 137.3 (s, CH). MS (EI): 246.1 (M^+).

1,2-Bis(4-methoxybenzyl)disulfane. Yield: 67%. ^1H NMR (400 MHz, $CDCl_3$): $\delta = 3.59$ (s, 4H, CH_2), 3.80 (s, 6H, OCH_3), 6.85 (d, $J_{HH} = 8.8$ Hz, CH, 4H), 7.17 ($J_{HH} = 8.8$ Hz, CH, 4H). ^{13}C NMR (400

MHz, $CDCl_3$): δ = 42.7 (s, CH_2), 55.3 (s, OCH_3), 113.9 (s, CH), 129.4 (s, C), 130.0 (s, C), 130.5 (s, CH). MS (EI): 306.1 (M^+).

1,2-Bis(2-methoxybenzyl)disulfane. Yield: 63%. ^{1}H NMR (400 MHz, $CDCl_3$): δ = 3.76 (s, 4H, CH_2), 3.86 (s, 6H, OCH_3), 6.85–6.92 (m, 4H, CH), 7.16 (dd, J_{HH} = 7.2 Hz, J_{HH} = 1.6 Hz, 2H, CH), 7.25 (dt, J_{HH} = 1.6 Hz, J_{HH} = 8.0 Hz, 4H, CH). ^{13}C NMR (400 MHz, $CDCl_3$): δ = 38.3 (s, CH_2), 55.5 (s, OCH_3), 110.6 (s, CH), 120.2 (s, CH), 125.8 (s, C), 128.8 (s, CH), 131.0 (s, CH), 157.4 (s, C). MS (EI): 306.1 (M^+).

1,2-Bis(1-phenylethyl)disulfane. Yield: 47%. A mixture of diastereomers. ^{1}H NMR (400 MHz, $CDCl_3$): δ = 1.54 (d, J_{HH} = 7.0 Hz, 3H, CH_3), 1.55 (d, J_{HH} = 7.0 Hz, 3H, CH_3), 3.52 (q, J_{HH} = 7.0 Hz, 1H, CH), 3.60 (q, J_{HH} = 7.0 Hz, 1H, CH), 7.21–7.34 (m, 10H, CH). ^{13}C NMR (400 MHz, $CDCl_3$): δ = 20.4 (s, CH_3), 20.5 (s, CH_3), 49.4 (s, CH), 49.5 (s, CH), 127.4 (s, CH), 127.5 (s, CH), 127.7 (s, CH), 127.8 (s, CH), 128.3 (s, CH), 128.4 (s, CH), 142.4 (s, C), 142.4 (s, C). MS (EI): 274.1 (M^+).

1,2-Bis(4-fluorobenzyl)disulfane. Yield: 41%. ^{1}H NMR (400 MHz, $CDCl_3$): δ = 3.58 (s, 4H, CH_2), 7.01 (dd, J_{HH} = 8.6 Hz, J_{HH} = 8.6 Hz, 4H, CH), 7.20 (dd, J_{HH} = 5.4 Hz, J_{HH} = 8.6 Hz, 4H, CH). ^{13}C NMR (400 MHz, $CDCl_3$): δ = 42.4 (s, CH_2), 115.4 (d, J_{CF} = 21.5 Hz, CH), 130.9 (d, J_{CF} = 8.1 Hz, CH), 133.1 (s, C), 162.2 (d, J_{CF} = 246.4 Hz, CF).

Di-*tert*-butyl((disulfanediylbis(methylene))bis(4,1-phenylene)) dicarbamate. Yield: 51%. ^{1}H NMR (400 MHz, $CDCl_3$): δ = 1.51 (s, 18H, CH_3), 3.58 (s, 4H, CH_2), 6.46 (br. s., 2H, NH), 7.15 (d, J_{HH} = 8.0 Hz, CH, 4H), 7.31 (d, J_{HH} = 8.0 Hz, 4H, CH). ^{13}C NMR (400 MHz, $CDCl_3$): δ = 28.3 (s, CH_3), 42.8 (s, CH_2), 118.4 (s, CH), 130.0 (s, CH), 131.8 (s, C), 137.6 (s, C), 152.6 (s, C).

DFT calculations

The calculations were carried out using the GAMESS (US) program package;[45] their results were visualized with the MacMolPlt graphical interface.[46] The poly(heptazine imide) matrix was modelled by a cluster comprising 6 heptazine units linked by 4 =NH groups and 2 N atoms. Two K^+ cations were added to neutralize the negative charge of the matrix, which originated from the deprotonated imide nitrogen atoms. To reduce computational cost, the symmetry of the model cluster was set to the C_{2v} point group. The basis was a Dunning–Hay double zeta set with one p-type polarization function on hydrogen atoms and one d-type function on other atoms. For the nitrogen atoms the basis set was additionally extended by a diffuse sp-shell. The geometry of K-PHI was optimized using 2 pure GGA functionals (PBE and BLYP) and 3 hybrids with different amounts of Hartree–Fock exchange (25% for PBE0, 20% for B3LYP and 50% for BHHLYP). The spatial distribution of the frontier orbitals in the cluster was found to be independent of the functional. On the other hand, the increase of the Hartree–Fock exchange percentage in the GGA < B3LYP < PBE0 < BHHLYP series increases the HOMO–LUMO gap by lowering the HOMO and raising the LUMO energies (see Table 1).

Conflicts of interest

There are no conflicts to declare.

Acknowledgements

The authors are grateful to the Deutsche Forschungsgemeinschaft for the financial support (DFG-An 156 13-1) and thank Christian Wolff for measuring time-resolved PL spectra. A. M. acknowledges the financial support from the scholarship of the President of Ukraine for young scientists. Computing resources for DFT calculations were provided by the SCIT supercomputer (V. M. Glushkov Institute of Cybernetics of the NAS of Ukraine).[47]

Notes and references

‡ Due to the M+ effect of the methoxy group, the oxidation potential of *p*-methylanisole is expected to be lower than that of toluene, 2.26 ± 0.02 V *vs.* SCE.[29] Alcohols, commonly used holes scavengers, cannot be applied in this case as they were reported to react with MV^{2+}.[48]

1 J. A. Labinger and J. E. Bercaw, *Nature*, 2002, **417**, 507–514.
2 G. Zhang, Z.-A. Lan and X. Wang, *Angew. Chem., Int. Ed.*, 2016, **55**, 15712–15727.
3 J. Zhang, M. Zhang, R.-Q. Sun and X. Wang, *Angew. Chem., Int. Ed.*, 2012, **51**, 10145–10149.
4 Z. Lin and X. Wang, *Angew. Chem., Int. Ed.*, 2013, **52**, 1735–1738.
5 L. Lin, C. Wang, W. Ren, H. Ou, Y. Zhang and X. Wang, *Chem. Sci.*, 2017, **8**, 5506–5511.
6 Y. Zheng, L. Lin, X. Ye, F. Guo and X. Wang, *Angew. Chem., Int. Ed.*, 2014, **53**, 11926–11930.
7 R. Kuriki, O. Ishitani and K. Maeda, *ACS Appl. Mater. Interfaces*, 2016, **8**, 6011–6018.
8 F. Guo, P. Yang, Z. Pan, X.-N. Cao, Z. Xie and X. Wang, *Angew. Chem., Int. Ed.*, 2017, **56**, 8231–8235.
9 A. E. Shilov and G. B. Shul'pin, in *Activation and Catalytic Reactions of Saturated Hydrocarbons in the Presence of Metal Complexes*, Kluwer Academic Publishers, 2000, ch. 1.
10 Y. Wang, H. Li, J. Yao, X. Wang and M. Antonietti, *Chem. Sci.*, 2011, **2**, 446–450.
11 S. Verma, R. B. N. Baig, M. N. Nadagouda and R. S. Varma, *ACS Sustainable Chem. Eng.*, 2016, **4**, 2333–2336.
12 A. Henríquez, H. D. Mansilla, A. M. M.-d. l. Cruz, J. Freer and D. Contreras, *Appl. Catal., B*, 2017, **206**, 252–262.
13 M. A. Gonzalez, S. G. Howell and S. K. Sikdar, *J. Catal.*, 1999, **183**, 159–162.
14 D. Dontsova, S. Pronkin, M. Wehle, Z. Chen, C. Fettkenhauer, G. Clavel and M. Antonietti, *Chem. Mater.*, 2015, **27**, 5170–5179.
15 A. Savateev, S. Pronkin, J. D. Epping, M. Willinger, C. Wolff, D. Neher, M. Antonietti and D. Dontsova, *ChemCatChem*, 2017, **9**, 167–174.
16 X. Wang, K. Maeda, A. Thomas, K. Takanabe, G. Xin, J. M. Carlsson, K. Domen and M. Antonietti, *Nat. Mater.*, 2009, **8**, 76–80.
17 A. Savateev, S. Pronkin, J. D. Epping, M. G. Willinger, M. Antonietti and D. Dontsova, *J. Mater. Chem. A*, 2017, **5**, 8394–8401.
18 A. Savateev, D. Dontsova, B. Kurpil and M. Antonietti, *J. Catal.*, 2017, **350**, 203–211.

19 B. Kurpil, K. Otte, M. Antonietti and A. Savateev, *Appl. Catal., B*, 2018, **228**, 97–102.
20 B. Kurpil, B. Kumru, T. Heil, M. Antonietti and A. Savateev, *Green Chem.*, 2018, **20**, 838–842.
21 B. Kurpil, A. Savateev, V. Papaefthimiou, S. Zafeiratos, T. Heil, S. Özenler, D. Dontsova and M. Antonietti, *Appl. Catal., B*, 2017, **217**, 622–628.
22 R. Godin, Y. Wang, M. A. Zwijnenburg, J. Tang and J. R. Durrant, *J. Am. Chem. Soc.*, 2017, **139**, 5216–5224.
23 V. W.-h. Lau, D. Klose, H. Kasap, F. Podjaski, M.-C. Pignié, E. Reisner, G. Jeschke and B. V. Lotsch, *Angew. Chem.*, 2016, **56**, 510–514.
24 F. Podjaski, J. Kröger and B. V. Lotsch, *Adv. Mater.*, 2018, **30**, 1705477.
25 Z. Chen, A. Savateev, S. Pronkin, V. Papaefthimiou, C. Wolff, M. G. Willinger, E. Willinger, D. Neher, M. Antonietti and D. Dontsova, *Adv. Mater.*, 2017, **29**, 1700555.
26 A. Savateev, S. Pronkin, M. Willinger, M. Antonietti and D. Dontsova, *Chem.–Asian J.*, 2017, **12**, 1517–1522.
27 G. Zhang, G. Li, Z.-a. Lan, L. Lin, A. Savateev, T. Heil, S. Zafeiratos, X. Wang and M. Antonietti, *Angew. Chem., Int. Ed.*, 2017, **56**, 13445–13449.
28 T. Watanabe and K. Honda, *J. Phys. Chem.*, 1982, **86**, 2617–2619.
29 P. B. Merkel, P. Luo, J. P. Dinnocenzo and S. Farid, *J. Org. Chem.*, 2009, **74**, 5163–5173.
30 A. M. Roy, G. C. De, N. Sasmal and S. S. Bhattacharyya, *Int. J. Hydrogen Energy*, 1995, **20**, 627–630.
31 M. Bouroushian, in *Monographs in Electrochemistry*, Springer-Verlag, Berlin Heidelberg, 2010, vol. 1, ch. 1, pp. 57–75.
32 G. Kutney, *Sulfur. History, Technology, Applications and Industry*, ChemTec Publishing, 2007.
33 W. J. Chung, J. J. Griebel, E. T. Kim, H. Yoon, A. G. Simmonds, H. J. Ji, P. T. Dirlam, R. S. Glass, J. J. Wie, N. A. Nguyen, B. W. Guralnick, J. Park, Á. Somogyi, P. Theato, M. E. Mackay, Y.-E. Sung, K. Char and J. Pyun, *Nat. Chem.*, 2013, **5**, 518–524.
34 J. Lim, J. Pyun and K. Char, *Angew. Chem.*, 2015, **54**, 3249–3258.
35 R. Ballini, *Synthesis*, 1982, **1982**, 834–836.
36 K. L. Stensaas, A. S. Brownell, S. Ahuja, J. K. Harriss and S. R. Herman, *J. Sulfur Chem.*, 2008, **29**, 433–443.
37 A. U. Meyer, V. W.-h. Lau, B. König and B. V. Lotsch, *Eur. J. Org. Chem.*, 2017, **2017**, 2179–2185.
38 A. J. Kamyshny, A. Goifman, J. Gun, D. Rizkov and O. Lev, *Environ. Sci. Technol.*, 2004, **38**, 6633–6644.
39 B. Eckert and R. Steudel, in *Elemental Sulfur und Sulfur-Rich Compounds II*, ed. R. Steudel, Springer Berlin Heidelberg, Berlin, Heidelberg, 2003, pp. 31–98, DOI: 10.1007/b13181.
40 A. M. d. P. Nicholas and D. R. Arnold, *Can. J. Chem.*, 1982, **60**, 2165–2179.
41 R. Breslow and J. L. Grant, *J. Am. Chem. Soc.*, 1977, **99**, 7745–7746.
42 T. Chivers and I. Drummond, *Inorg. Chem.*, 1972, **11**, 2525–2527.
43 T. Ishida, S. Kikuchi, T. Tsubo and T. Yamada, *Org. Lett.*, 2013, **15**, 848–851.
44 F. Goettmann, A. Fischer, M. Antonietti and A. Thomas, *Angew. Chem., Int. Ed.*, 2006, **45**, 4467–4471.
45 M. W. Schmidt, K. K. Baldridge, J. A. Boatz, S. T. Elbert, M. S. Gordon, J. H. Jensen, S. Koseki, N. Matsunaga, K. A. Nguyen, S. Su, T. L. Windus, M. Dupuis and J. A. Montgomery Jr, *J. Comput. Chem.*, 1993, **14**, 1347–1363.
46 B. M. Bode and M. S. Gordon, *J. Mol. Graphics Modell.*, 1998, **16**, 133–138.
47 A. L. Holovynsky, A. L. Malenko and I. V. Sergienko, *Visn. Nac. Akad. Nauk Ukr.*, 2013, 50–59.
48 J. G. Carey, J. F. Cairns and J. E. Coxhewer, *J. Chem. Soc. D*, 1969, 1280–1281.